

Practically Perfect Hindcasts of Severe Convective Storms

Vittorio A. Gensini, Alex M. Haberlie, and Patrick T. Marsh

ABSTRACT: This study presents and examines a modern climatology of U.S. severe convective storm frequency using a kernel density estimate to showcase various aspects of climatological risk. Results are presented in the context of specified event probability thresholds that correspond to definitions used at the NOAA/NWS's Storm Prediction Center following a practically perfect hindcast approach. Spatial climatologies presented herein are closely related to previous research. Spatiotemporal changes were examined by splitting the study period (1979–2018) into two 20-yr epochs and calculating deltas. Portions of the southern Great Plains and High Plains have seen a decrease in counts of tornado event threshold probability, whereas increases have been documented in the middle Mississippi River valley region. Large hail, and especially damaging convective wind gusts, have shown increases between the two periods over a majority of the CONUS. To temporally showcase local climatologies, event threshold days are shown for 12 select U.S. cities. Finally, data created and used in this study are available as an open-source repository for future research applications.

<https://doi.org/10.1175/BAMS-D-19-0321.1>

Corresponding author: Vittorio A. Gensini, vgensini@niu.edu

In final form 23 January 2020

©2020 American Meteorological Society

For information regarding reuse of this content and general copyright information, consult the [AMS Copyright Policy](#).

From 1980 to 2005, severe convective storms¹ (SCSs) resulted in average economic losses of 2.3 billion consumer price index (CPI) adjusted U.S. dollars per year (NCEI 2020). In the last 13 years (2006–18), damages from SCSs have averaged 13.6 billion CPI adjusted dollars per year, increasing 591% from the previous 26-yr period. The upward trend in SCS losses (especially since the mid-2000s) has generated great interest from stakeholders and researchers (Simmons and Sutter 2013; Smith and Matthews 2015). Discussions about trend attribution are often framed around recent research on growth in the human built environment (i.e., exposure) and potential changes in SCS frequency/variability due to anthropogenic climate change. Potential hypotheses for these changes could be broadly broken down into four general categories: 1) increases in losses are primarily due to increases in the extent of the built environment, 2) increases in losses are primarily due to changes in the climatology of SCS frequency, 3) increases in losses are equally due to changes in the built environment and changes in SCS frequency, or 4) other, potentially unknown, factors are responsible for the observed trends in U.S. SCS losses.

While this is a difficult research question to fully answer, several important studies have provided insight on various aspects of these hypotheses. For example, in regard to exposure and the built environment, changes in land use leading to the expansion of urban and suburban metropolitan districts can greatly increase the likelihood of a tornado disaster (Ashley et al. 2014; Rosencrants and Ashley 2015; Strader and Ashley 2015; Ashley and Strader 2016; Strader et al. 2017a). Tornado disasters are likely to increase in the future, even if the climatological frequency of U.S. tornadoes remains unchanged (Strader et al. 2017b). Less work has been done in this realm for other aspects of SCS events (i.e., large hail and damaging convective wind gusts), but it should follow that conclusions from such studies would largely remain unchanged. This has been demonstrated by other work focusing on the hazards of wildfires (Strader 2018), hurricanes (Freeman and Ashley 2017), and inland flooding (Ferguson and Ashley 2017).

¹ U.S. SCS events are defined as a hailstone ≥ 2.5 cm in diameter, a tornado of any strength, or a thunderstorm-induced wind gust $\geq 2.5 \text{ m s}^{-1}$.

These, and other, studies frequently utilize historical archives of hazard information as input into the assessment of risk associated with a specific natural hazard. For SCS events, this historical database extends back to the early 1950s and serves as a basis for SCS climatological studies. Due to the importance of historical SCS risk assessments for assessing future change, this study seeks to 1) update the results of many previous works on U.S. SCS climatology, 2) present novel findings to stakeholders and users of the U.S. SCS database for purposes of better assessing the risk associated with these natural hazards, and 3) introduce an open-source hindcast dataset for users wishing to perform their own SCS climatological analyses.

Background

Numerous studies have reported on and confirmed various aspects related to the climatology of SCS events in the United States. Estimation of tornado probabilities at point locations have been examined for decades, and have served as the foundation for estimates of local tornado risk (Thom 1963; Kelly et al. 1978; Brooks et al. 2003; Krocak and Brooks 2018). A recent review related to various aspects of tornado climatology can be found in Moore and DeBoer (2019). Hail climatologies have also been examined, usually due to their economic importance (e.g., damage to agriculture and property). Previous research has examined mesoscale networks of hail pads (Changnon 1977), first-order observation stations (Changnon 1999; Changnon

and Changnon 2000; Changnon 2001), insurance claims (Changnon 2008), and radar or satellite-derived estimates (Cintineo et al. 2012; Cecil and Blankenship 2012) to assess hail climatologies. Further reading about the U.S. hail climatology can be found in a recent review by Allen and Tippett (2015). For damaging convective wind gusts, climatological results are muddled. This is often due to the differences in report origin (estimated vs measured), report source (e.g., trained weather spotter, emergency manager, public), and potential for different degrees of damage depending on environmental circumstances and the object impacted (Trapp et al. 2006; Smith et al. 2013; Edwards et al. 2018). Studies have been cautious with the interpretation and overall utility of SCS reports while noting they are the best ground-truth data currently available for such climatological research.

Temporally, the average annual number of U.S. tornado reports more than doubles over the lifetime of the modern SCS record (1950–present), with most of this increase associated with weak tornadoes (those rated EF0 on the enhanced Fujita scale; Doswell et al. 2009). Likewise, U.S. hail and damaging convective wind gust reports have increased by an order of magnitude through the same reporting period (Tippett et al. 2015). Increases in all SCS hazards appear to be nonmeteorological in origin (Verbout et al. 2006; Allen and Tippett 2015; Edwards et al. 2018). However, there are aspects of SCS reports that are less affected by such nonmeteorological factors. Examples include annual significant tornado frequency (those rated EF2 or greater), the number of annual days with significant hail reports (diameter $\geq \approx 5$ cm), and measured severe convective wind gusts (Allen and Tippett 2015; Tippett et al. 2015; Edwards et al. 2018). For tornadoes, the aggregate consensus indicates that frequency has remained relatively constant through the most reliable portions of the climatological record (Verbout et al. 2006; Kunkel et al. 2013; Tippett et al. 2015; Long et al. 2018; Potvin et al. 2019). Trends have been noted, however, in the temporal variability (Brooks et al. 2014; Tippett 2014; Farney and Dixon 2015; Guo et al. 2016) and spatial locations of tornado (Gensini and Brooks 2018; Moore and McGuire 2019) and hail (Tang et al. 2019) reports. A more clear consensus about spatiotemporal trends in damaging convective wind gusts has yet to emerge in the literature.

In addition to reports, other studies have utilized the background convective environment as a proxy for SCS frequency. This has typically resulted in the formation of spatial–statistical models using various forms of regression techniques. As an example, Poisson regression has demonstrated skill in explaining the variance associated with monthly tornado frequency by using an observation-based covariate of monthly averaged atmospheric parameters (Tippett et al. 2012, 2014). A Bayesian hierarchical approach and an inhomogeneous Poisson process have also been used to explain the variance of tornado frequency at various spatiotemporal scales using convective environments (Cheng et al. 2016; Gensini and Bravo de Guenni 2019). Similar work has also been done over North America for large hail reports in an attempt to estimate hailstone diameter and/or frequency from the preconvective environment (Jewell and Brimelow 2009; Allen et al. 2015).

Although not the focus of this study, diagnosing the potential for future change in SCS events has recently become an area of interest for research. Through use of global climate models, much of this focus has been on atmospheric environments known to be favorable (Brooks et al. 1994, 2003; Brooks and Dotzek 2008; Gensini and Ashley 2011) for the development of SCS events (Del Genio et al. 2007; Marsh et al. 2007; Trapp et al. 2007; Diffenbaugh et al. 2013; Gensini et al. 2014) given the current coarse horizontal grid spacing of global climate models. However, recent work has also examined the use of high-resolution dynamical downscaling (Gensini and Mote 2015; Hoogewind et al. 2017; Trapp et al. 2019), the “pseudo global warming” approach (Trapp and Hoogewind 2016), and 1D cloud models (Brimelow et al. 2017) for purposes of assessing potential future changes in various SCS phenomena. These studies suggest that future SCS events may be more frequent in the future due to an increasing number days with favorable SCS ingredients (Brooks 2013; Tippett et al. 2015). Increases in

future interannual variability of SCS events have also been suggested (Gensini and Mote 2015; Hoogewind et al. 2017), but it is still unclear as to what might be driving such results, especially considering several studies have already documented a notable increase in interannual variability (Brooks et al. 2014; Tippett 2014; Farney and Dixon 2015; Guo et al. 2016).

Given the importance of SCS climatological data for nearly all of the studies discussed above, this study seeks to compile and present SCS information in a novel way that is easy to comprehend to a general audience. To do so, we have developed a climatological database of SCS activity that is focused on methods using “perfect” hindcasts first described by previous research (Hitchens and Brooks 2012; Hitchens et al. 2013; Hitchens and Brooks 2014). The result of our work is a gridded compilation of SCS hindcasts that are relatively easy to understand for any person who has inspected SPC convective outlooks.

Methodology

Data on SCS reports were obtained from the National Centers for Environmental Information (NCEI) Storm Data (Schaefer and Edwards 1999) record for the period 1979–2018. This 40-yr period of analysis is consistent with the most reliable portion of the U.S. SCS database despite some documented issues. For instance, it is well known that SCS observations are sensitive to spatial and nonmeteorological biases relating to variations in population, measurement estimation, and other discontinuities in the record (Verbout et al. 2006; Potvin et al. 2019). Three important notes about the data presented in this study include 1) all tornadoes (regardless of EF rating) were used, 2) all wind reports with no estimated or measured value in the Storm Data report field were omitted from the study, and 3) the NWS criterion for severe hail changed from 0.75 to 1 in. diameter in 2010. Hail reports were considered as SCS events if they met the defined NWS criterion during their respective epoch (i.e., pre- or post-2010). Finally, readers should note that there was a procedural database change for wind in 1996 that required local NWS offices to record either a wind speed or damage value. This is an important change to note when examining a U.S. time series of damaging convective wind gust frequency.

SCS reports were aggregated at daily (1200–1200 UTC) intervals and used to calculate practically perfect hindcast (PPH) probabilities of individual SCS hazards on NCEP’s 211 Lambert-conformal grid (approximately 80-km horizontal grid spacing). PPH calculations follow Eq. (1) in Hitchens et al. (2013):

$$\text{PPH} = \sum_{n=1}^N \frac{1}{2\pi\sigma^2} \exp\left[-\frac{1}{2}\left(\frac{d_n}{\sigma}\right)^2\right], \quad (1)$$

where d_n is the Euclidean distance from the grid point to the n th location that had an SCS report, N is the total number of grid points with SCS reports, and σ is a weighting function that can be interpreted as the confidence one has in the location of the SCS event. The σ value was set to 1.5 in this study, as this has been shown to optimally represent verification of operational SCS forecasts from the NOAA/NWS’s Storm Prediction Center (SPC) (Hitchens et al. 2013). This PPH calculation closely matches the probabilistic outlook methodology used by the SPC, which is to forecast probabilities of SCS events within 25 mi of a point. PPH values were then bilinearly interpolated to NCEP’s 212 Lambert-conformal grid (approximately 40-km horizontal grid spacing) to increase granularity of the climatological analysis.

The basic premise of PPH is to construct probabilities of event occurrence based on SCS reports. This is accomplished by spatially smoothing SCS reports using a Gaussian filter. Smoothing helps recreate the uncertainty that typically exists at the outlook forecast stage and creates a hindcast that perfectly represents the observed outcome. In other words, PPH probabilities offer a consistent, objective representation of what a perfect SPC forecast may have looked like for a particular forecast event. Recent research has also utilized practically

perfect probabilities as a verification metric for verifying SCS forecasts from a numerical weather prediction model (Gensini and Tippett 2019).

For each SCS hazard, attributes of the PPH fields (e.g., areal coverage of a probability threshold) were assembled by year and month for climatological comparison. Each grid was first thresholded by five different probabilities—5%, 15%, 30%, 45%, 60%—corresponding to thresholds used by the SPC for day 1 hail and convective wind gust forecasts. For interhazard consistency, the 2% and 10% thresholds used by the SPC for tornadoes only were not examined. The process was repeated for significant severe convective storms (i.e., hailstones ≥ 5 cm in diameter, a tornado of \geq EF2 magnitude, or a thunderstorm-induced wind gust

$\geq 33 \text{ m s}^{-1}$) to uniquely examine these extreme events. A PPH threshold of 10% was used for significant severe weather following operational definitions of “hatched” areal outlooks used at the SPC. While it is convenient to interchange PPH thresholds with SPC forecast thresholds, readers must exercise caution in their comparison as they represent mutually exclusive aspects of the forecast process (e.g., forecast vs a hindcast). This was demonstrated by examining the relationship of SPC convective outlook area to storm report area by year, which showed that forecast skill has changed through time (Hitchens and Brooks 2012).

Grids were compiled and stored as netCDF files (available for download at <http://atlas.niu.edu/pperfect/BAMS/>) in an effort to create an open-source repository for other users. Results presented in this article are based on the number of times (i.e., how many days) a grid cell was activated during a given period. For areal calculations, a simplified grid cell size of $1,600 \text{ km}^2$ ($40 \text{ km} \times 40 \text{ km}$) is used to communicate the areal extent of PPH coverage.

Results

Spatial distribution. PPH “SLIGHT” RISKS. Annual counts of PPH days exceeding the SPC “slight” risk categorical threshold were examined first by creating an average count value over the 40-yr (1979–2018) period. These thresholds correspond to 5%, 15%, and 15% for tornado, hail, and wind, respectively (more information about the conversion of SPC probabilistic forecasts to subjective categories can be found at www.spc.noaa.gov/misc/SPC_probotlk_info.html). Gridpoint days meeting or exceeding more than one PPH hazard threshold were only counted once. Across the CONUS, the maximum corridor for these frequencies extends $\approx 200 \text{ km}$ on either side of a line from Hays, Kansas, to Oklahoma City, Oklahoma (Fig. 1a). This area

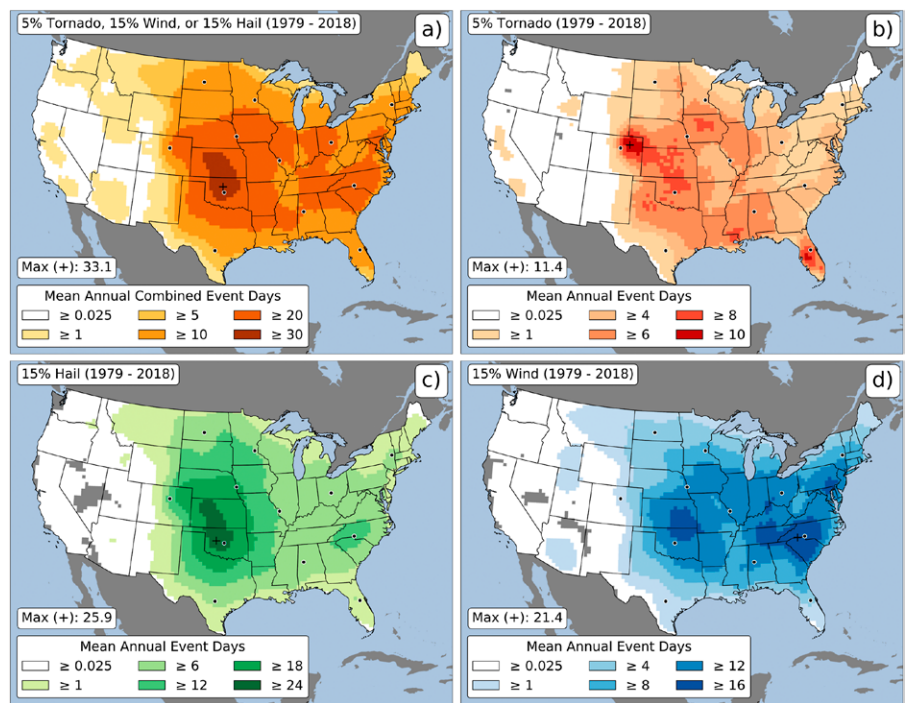


Fig. 1. Mean annual count of days (1200–1200 UTC) from 1979 to 2018 meeting or exceeding a practically perfect probability of (a) 5% for tornado reports, 15% for hail reports, or 15% for wind reports, (b) 5% for tornado reports, (c) 15% for hail reports, and (d) 15% for wind reports. The gray areas over the CONUS denote regions where no events occurred during the study period. The black plus signs denote the location of the maximum mean annual event day count. The selected cities in (a) are (i) Bismarck, (ii) Minneapolis, (iii) Albany, (iv) Omaha, (v) Columbus, (vi) Denver, (vii) St. Louis, (viii) Charlotte, (ix) Oklahoma City, (x) Tuscaloosa, (xi) San Antonio, and (xii) Orlando.

experiences ≥ 30 days per year with PPH values verifying the “slight” risk categorical threshold used by the SPC. Most grid points east of the Continental Divide experience at least 5 days per year with a PPH value from tornado, wind, or hail that would verify the “slight” risk threshold.

For tornadoes, greatest frequencies are found in northeast Colorado, with an average of at least 10 days per year with a PPH value of 5% (Fig. 1b). Local maxima are also noted in the central Great Plains, central Iowa, central Florida, and southern Mississippi. A “C” shaped pattern is noted in the central CONUS corresponding to at least 6 days per year with a 5% tornado PPH value. West of the Rocky Mountains, local maxima are noted in central/Southern California and southeast Idaho. These results closely match point-density estimates of daily tornado probabilities published in Brooks et al. (2003).

Hail produces the greatest number of PPH “slight” risks per year (Fig. 1c). A maximum of ≈ 26 days per year is found just west-northwest of Oklahoma City. The spatial extent of maximum values tallying at least 24 days per year is similar to the corridor of greatest frequencies found in Fig. 1a. Mean annual event days decrease outside of this area, with most of the central and eastern CONUS experiencing an average of at least 6 days per year. A local maximum of 12 days per year is noted in the western Carolinas, while PPH “slight” risks are very rare (<1 per year) west of the Continental Divide. Overall, hail results show the importance of close proximity to the greatest climatological frequencies of the elevated mixed layer, which is a significant contributor to favorable hail environments through the generation of steep midlevel lapse rates (Carlson et al. 1983; Lanicci and Warner 1991, 1997; Banacos and Ekster 2010).

PPH “slight” risks for wind exhibit a distinctly different spatial pattern (Fig. 1d). An annual average maximum of 21.4 days per year is found just southwest of Charlotte, North Carolina, in a corridor of higher counts throughout portions of North Carolina, South Carolina, Tennessee, and Kentucky. Again, included here are both measured and estimated gusts $\geq \approx 25 \text{ m s}^{-1}$, which are known to introduce errors into the wind database (Trapp et al. 2006; Smith et al. 2013; Edwards et al. 2018). Given these, and other, issues with this aspect of the SCS database, we have lower confidence in the spatial distributions and magnitudes herein. This will be further elaborated on when examining significant severe convective wind gusts, which appear to be less impacted by nonmeteorological factors.

PPH “MODERATE” RISKS. Analyzed next were the 40-yr average count values for PPH 30% tornado, 60% hail, and 60% wind. When not considering mutual probabilities of significant severe weather, these are the first probabilistic thresholds used by the SPC to define a “moderate” categorical risk. At least 12 days per year reach this threshold in a small corridor from Oklahoma City to Wichita, Kansas (Fig. 2a), driven by high relative frequencies from 30% tornado (Fig. 2b) and especially 60% hail (Fig. 2c). In fact, hail is responsible for an average of at least 8 PPH “moderate” days per year in central Kansas and central Oklahoma. 30% PPH tornado probabilities are extremely rare west of the Rocky Mountains, with several states (Washington, Oregon, Nevada, and Utah) having never recorded such a value. 60% wind PPH values (Fig. 2d) show a similar spatial pattern to the 15% distribution (Fig. 1d), but perhaps with even a stronger signal for the influence of nonmeteorological factors. Relative spatial maxima are found in the Ohio Valley, Tennessee Valley, and mid-Atlantic regions. Readers are again cautioned to interpret convective wind gust results in these areas versus other regions due to a higher propensity for estimated wind gusts from tree damage. Other relative patterns for 60% PPH wind values (e.g., Corn Belt, southeast Kansas) correspond befittingly with previous research examining derecho climatologies (Bentley and Mote 1998, 2000; Coniglio and Stensrud 2004; Ashley and Mote 2005).

PPH SIGNIFICANT SEVERE. Finally, spatial analyses of PPH values were conducted using 10% probabilities of significant severe weather. This threshold corresponds to the “hatching”

used in by SPC in their operational probabilistic SCS hazard outlooks. Significant severe weather reports are often utilized heavily for climatological SCS studies because of their tendency to be less impacted by nonmeteorological factors (Tippett et al. 2015). If one wanted to live in the peak location of significant severe weather climatological frequency in the United States, then that city would be Dodge City, Kansas, experiencing an average of at least 8 days per year verifying a “hatching” forecast (Fig. 3a). A large area of at least 4 days per year extends from north-central Texas northward through Oklahoma and Kansas, then eastward through central-eastern Nebraska, Iowa, and northern Illinois.

Tornado PPH “hatching” days are most common in a circle shape around the state of Missouri, with highest frequencies found in eastern Oklahoma, southern Arkansas, central Mississippi, northern Alabama, central Tennessee, and western Kentucky (Fig. 3b). West of the 105°W meridian—approximately the longitude of Denver, Colorado—most locations have never experienced a 10% tornado PPH value. Exceptions to this include north-central Wyoming, north-central Montana, northern Arizona, and California’s Southland coast. These areas recorded 1 event during the 40-yr study period.

Of all the SCS hazards, significant hail is the most geographically focused (Fig. 3c). The maximum frequency (≈ 5 days per year) of PPH hail “hatching” is found just southwest of Oklahoma City. Nearly all grid points in northern Texas, Oklahoma, Kansas, and Nebraska

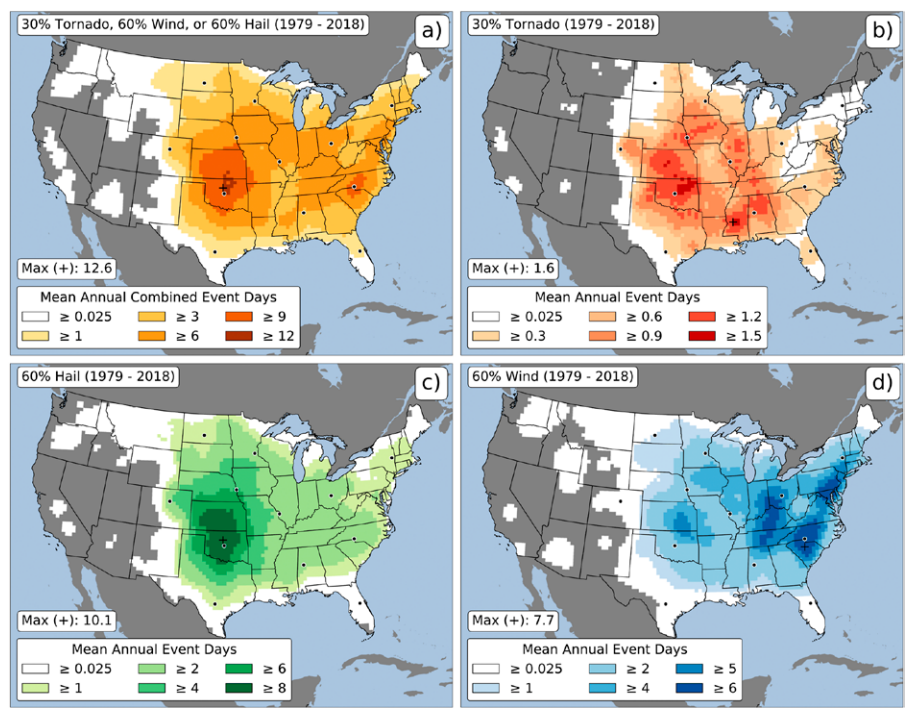


Fig. 2. As in Fig. 1, but for (a) 30% for tornado reports, 60% for hail reports, or 60% for wind reports, (b) 30% for tornado reports, (c) 60% for hail reports and (d) 60% for wind reports.

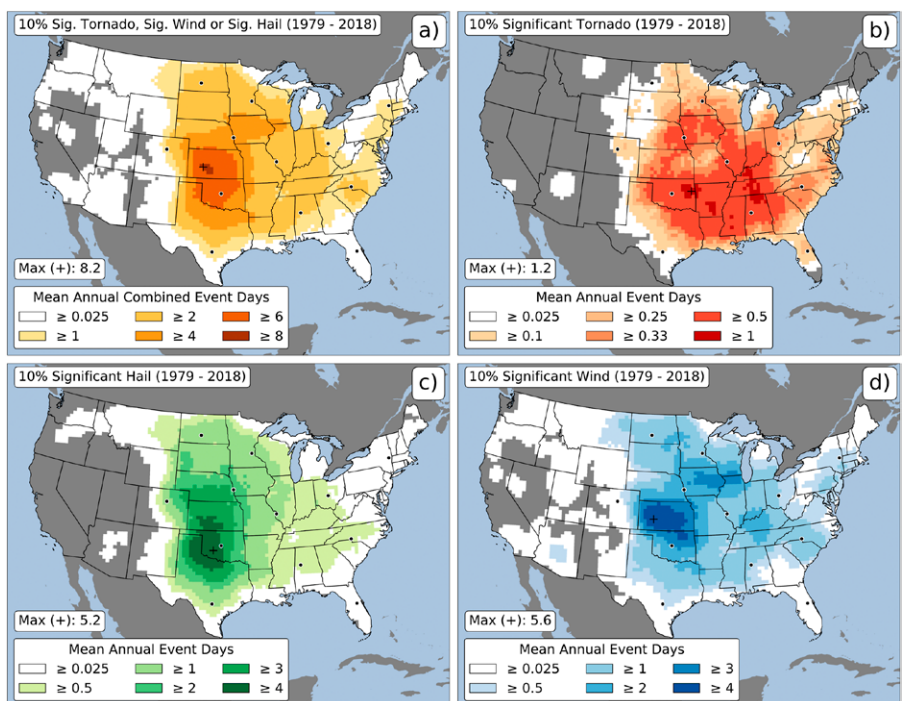


Fig. 3. As in Fig. 1, but for (a) 10% for significant tornado ($\geq EF2$), significant hail (≥ 5.08 cm), or significant wind (333.4 m s^{-1}) reports, (b) 10% for significant tornado reports, (c) 10% for significant hail reports, and (d) 10% for significant wind reports.

experience at least 2 PPH 10% days from significant hail per year. Annual average counts have a sharp gradient on the western edge of the maximum areas (tied to the elevation of the Rocky Mountains), and a more gradual decrease as one moves east from the spatial maximum. 10% PPH “hatching” for hail has never occurred during our study period in California, Nevada, or Utah.

Significant wind PPH frequencies show an interesting distribution, especially when compared to Fig. 2d. On average, central Kansas records the highest frequency of PPH wind “hatching” days (at least 4 per year; Fig. 3d). Another relative maximum is noted in central-eastern Iowa and northern Illinois, likely associated with the previously discussed climatology of derechos. The Tennessee Valley, Ohio Valley, and mid-Atlantic recorded at least 6 days per year with 60% PPH wind (Fig. 2d); however, these areas generally recorded less than 2 days per year with 10% PPH significant wind. West of the Continental Divide, south-central Arizona records a wind PPH “hatching” once every other year on average. This is likely related to the climatological maximum of thunderstorm-induced haboob storms (Idso et al. 1972).

Spatial changes. To examine potential temporal changes in the presented spatial climatologies, the 40-yr analysis period was split into two 20-yr epochs (1979–98 and 1999–2018). Average annual counts were then recreated for each 20-yr period to calculate epoch Δ values. 20-yr climatologies were first generated for the PPH “slight” risk days shown in Fig. 1. Their frequency has increased across most CONUS locations with the exception of portions of Florida, California, and the Great Basin (Fig. 4c) on the order of at least 2 additional days per year versus the previous 20-yr period. Examining tornadoes, an increase of 1–4 days per year is found in a broad area spanning either side of the Mississippi River valley (Fig. 4f). A maximum increase was found in western Kentucky of +4.4 days per year. Decreases in tornado PPH “slight” risk days are shown in all locations west of the Continental Divide, with other relative minima the I-25 corridor from Denver to Cheyenne, Wyoming, the northeast United States, Florida, and the Llano Estacado across the west Texas High Plains. Changes in these values mimic recent research highlighting spatial trends in U.S. tornado frequency (Gensini and Brooks 2018). Changes in PPH hail (Fig. 4i) and wind (Fig. 4l) “slight” risks have been upward in most areas, with wind showing the greatest magnitude of increase between hazards (nearly 36 more days per year on average vs the previous 20-yr period). In fact, most of the eastern one-third of the CONUS has exhibited at least 20 more days per year versus the previous 20-yr period, significantly driving the full-period distributions shown in Fig. 1d. Hail also shows an impressive relative maximum Δ , with at least 15 more days per year being reported in western Kansas, Nebraska, and southwest South Dakota versus the previous 20-yr period. This is consistent with recent research examining trends in U.S. hail reports and favorable hail environments (Tang et al. 2019).

The same epoch analysis was then performed for PPH significant severe weather, using the same 10% threshold as before (Fig. 5). Increases in significant hail and significant wind combine to create a total increase for any PPH “hatching” of at least 6 days per year in western Kansas versus the previous 20-yr period (Fig. 5c). PPH “hatching” for tornadoes exhibit the greatest decreases (~1 day every other year) across the southern Great Plains and the greatest increases in the middle–Mississippi Valley and mid-South (+1 day every other year). These tornado Δ values are again consistent with previous research on spatial trends in U.S. tornado activity (Gensini and Brooks 2018). On average, at least 2 more days per year with practically perfect hail “hatching” occurred in the second versus first epoch in a region to the right of a line from Oklahoma City to Dallas/Forth Worth, Texas, to Amarillo, Texas, to Denver, to Omaha, Nebraska, and back to Oklahoma City (Fig. 5i). Finally, PPH wind hatching was relatively uncommon east of the Mississippi River during the period 1979–98 (Fig. 5j).

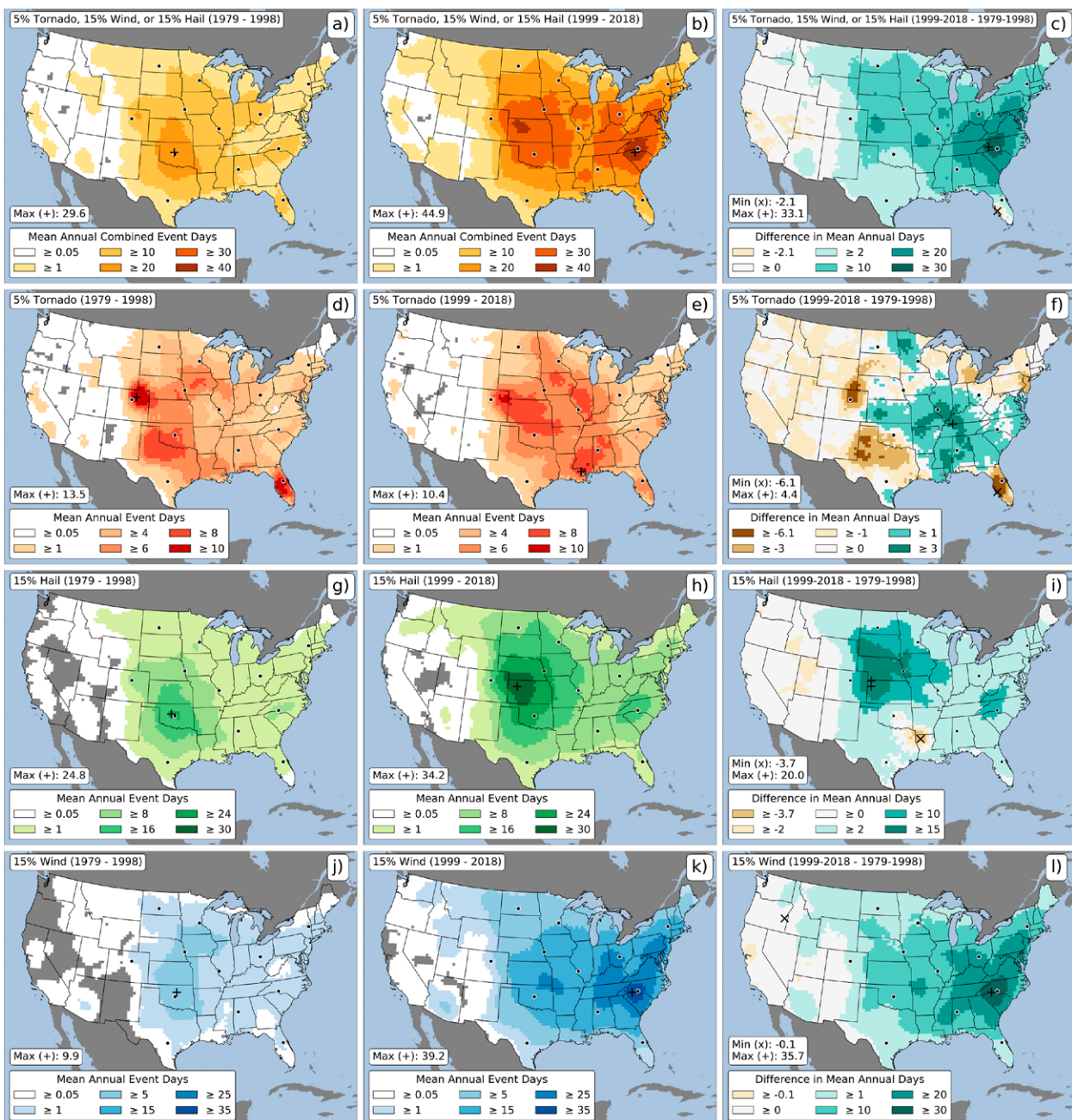


Fig. 4. As in Fig. 1, but for (a)–(c) 5% tornado reports, 15% hail reports, or 15% wind reports, (d)–(f) 5% tornado reports, (g)–(i) 15% hail reports, (j)–(l) 15% wind reports for (a),(d),(g),(j) 1979–98, (b),(e),(h),(k) 1999–2018, and (c),(f),(i),(l) the difference between the two periods.

Most places doubled or tripled their average annual count in the second epoch (Figs. 5k,l). This is also true in western Kansas, where an increase of +7.2 days per year has been found versus the previous 20-yr period. The causes of change are not well known at this time, but may be related to factors such as climate variability, anthropogenic climate change, reporting consistency, warning verification practices, or other nonmeteorological factors.

Annual risk for selected cities. To demonstrate how local municipalities (e.g., emergency managers) may utilize the database herein for risk analysis, counts of daily PPH exceedance were extracted and summed by year for a geographically diverse set of 12 U.S. cities: (i) Bismarck, North Dakota, (ii) Minneapolis, Minnesota, (iii) Albany, New York, (iv) Omaha, (v) Columbus, Ohio, (vi) Denver, (vii) St. Louis, Missouri, (viii) Charlotte, (ix) Oklahoma City, (x) Tuscaloosa, Alabama, (xi) San Antonio, Texas, and (xii) Orlando, Florida (locations marked in

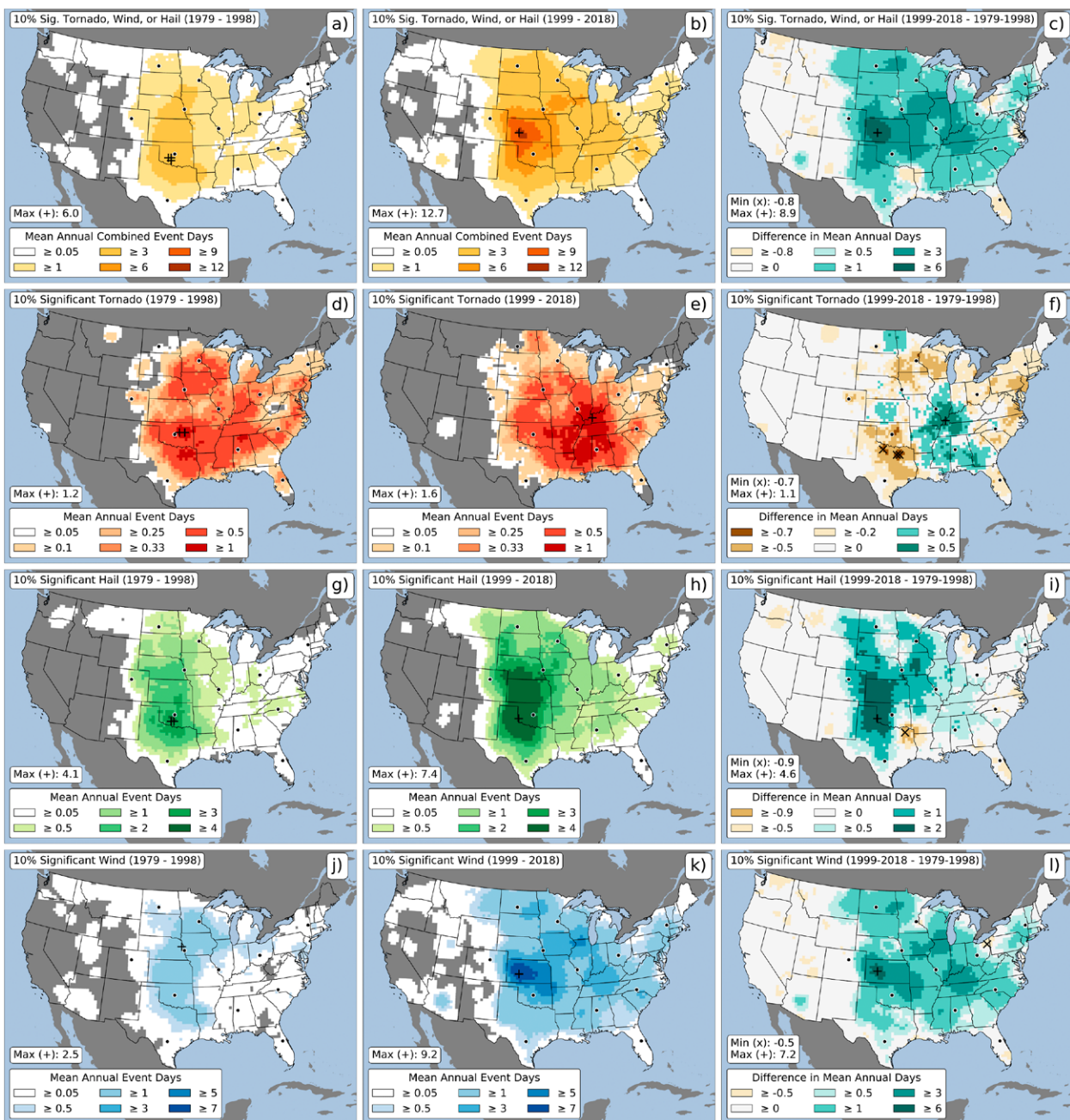
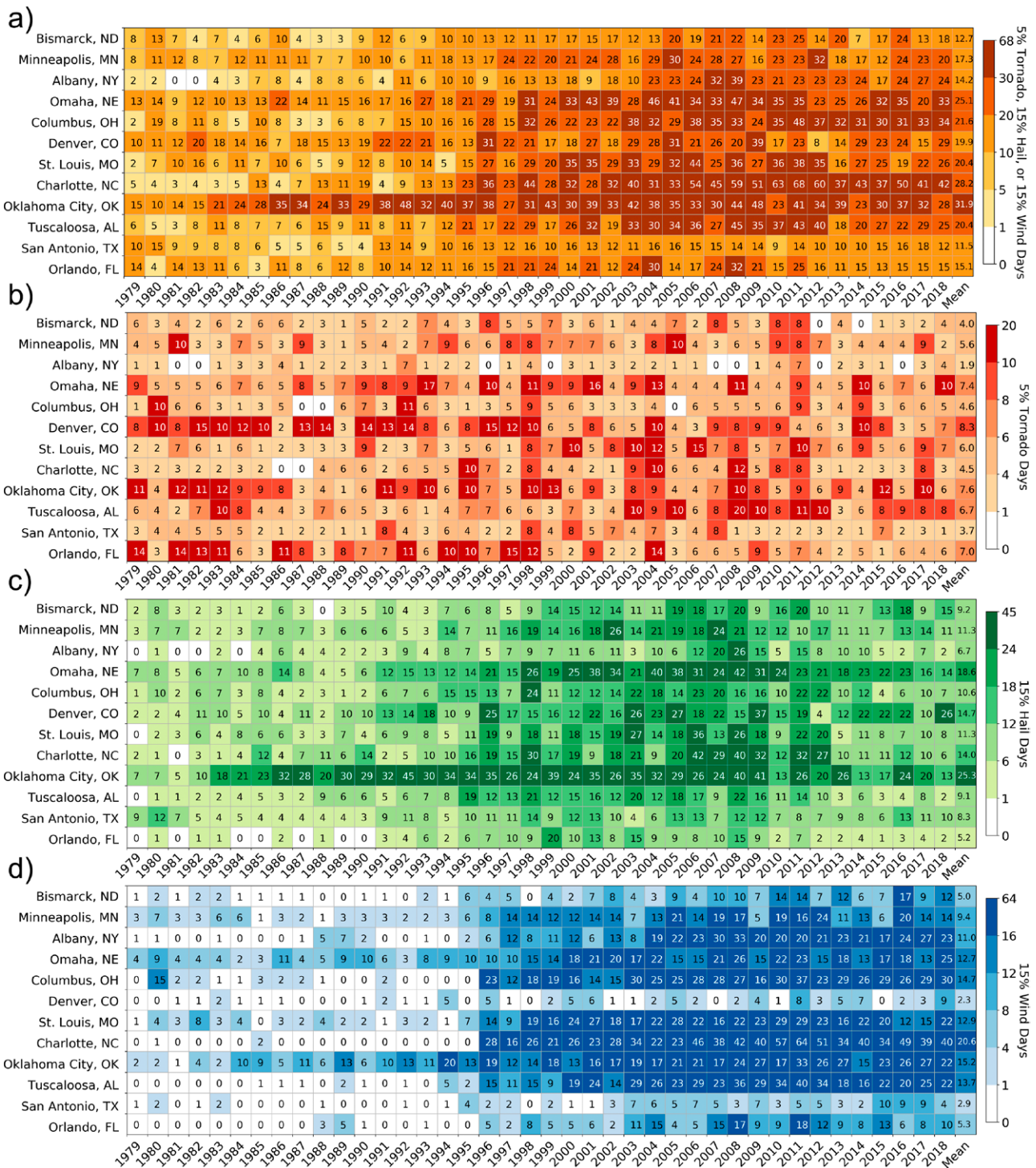


Fig. 5. As in Fig. 4, but for (a)–(c) 10% significant tornado reports, 10% significant hail reports, or 10% significant wind reports, (d)–(f) 10% significant tornado reports, (g)–(i) 10% significant hail reports, and (j)–(l) 10% significant wind reports.

Fig. 1a). Out of the cities examined, Oklahoma City has the highest average annual count (31.9 days) of any PPH “slight” risk (Fig. 6a). Also analyzed were the individual tornado (Fig. 6b), large hail (Fig. 6c), and damaging convective wind gust (Fig. 6d) PPH “slight” annual counts. Denver, Oklahoma City, and Charlotte lead the mean annual counts for tornado (8.3 days), large hail (25.3 days), and damaging convective wind gusts (20.6 days), respectively.

Except for tornadoes, one can see the significant increases in hail—but especially in damaging convective wind gust PPH “slight” events—in nearly all locations since ≈ 1996 . While the cause of this rapid increase is unknown, this temporal step change does coincide with the last modernization of the National Weather Service and a procedural change in the way damaging convective wind gust reports were recorded. For hail, consistent frequencies found for Oklahoma City may be related to the field programs and storm chasing activities that were more common there versus other cities throughout the 1980s and 1990s.



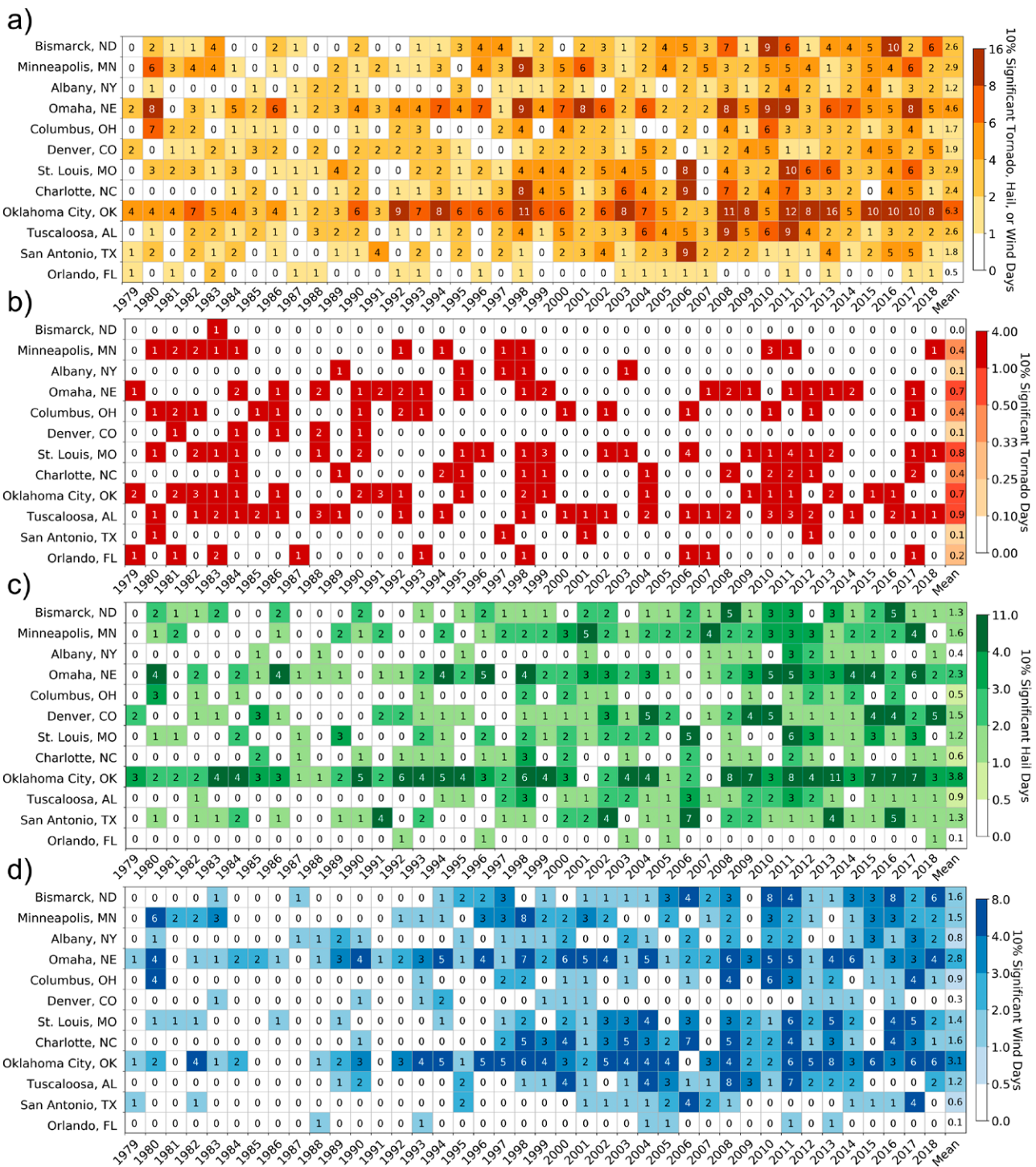


Table 1. Mean annual number of days (1979–2018) that meet or exceed selected practically perfect probability thresholds in each city's representative grid cell for tornadoes.

City	5% tornado	30% tornado	45% tornado	10% significant tornado
Bismarck, ND	4.1	0.1	0.0	0.0
Minneapolis, MN	5.6	0.8	0.4	0.4
Albany, NY	1.9	0.2	0.1	0.1
Omaha, NE	7.4	1.3	0.6	0.7
Columbus, OH	4.6	0.5	0.2	0.4
Denver, CO	8.3	0.7	0.2	0.2
St. Louis, MO	6.0	1.2	0.6	0.8
Charlotte, NC	4.5	0.5	0.3	0.4
Oklahoma City, OK	7.6	1.5	0.9	0.7
Tuscaloosa, AL	6.7	1.2	0.6	0.9
San Antonio, TX	3.7	0.4	0.2	0.1
Orlando, FL	7.1	0.4	0.2	0.3

Table 2. As in Table 1, but for hail.

City	15% hail	30% hail	60% hail	10% significant hail
Bismarck, ND	9.2	4.5	1.5	1.3
Minneapolis, MN	11.3	6.8	3.5	1.6
Albany, NY	6.7	4.0	1.9	0.4
Omaha, NE	18.6	11.1	5.8	2.3
Columbus, OH	10.6	5.8	2.5	0.5
Denver, CO	14.7	7.9	3.4	1.5
St. Louis, MO	11.3	6.7	3.4	1.2
Charlotte, NC	14.0	8.0	3.3	0.6
Oklahoma City, OK	25.3	17.0	9.5	3.8
Tuscaloosa, AL	9.1	5.6	2.6	0.9
San Antonio, TX	8.4	4.5	1.8	1.3
Orlando, FL	5.2	1.9	0.5	0.1

Table 3. As in Table 1, but for wind.

City	15% wind	30% wind	60% wind	10% significant wind
Bismarck, ND	5.0	2.4	0.9	1.6
Minneapolis, MN	9.5	5.9	3.3	1.5
Albany, NY	11.0	7.5	4.5	0.8
Omaha, NE	12.7	7.5	3.7	2.8
Columbus, OH	14.7	9.5	5.3	0.9
Denver, CO	2.3	0.6	0.2	0.3
St. Louis, MO	12.9	7.9	4.1	1.4
Charlotte, NC	20.6	14.0	7.3	1.6
Oklahoma City, OK	15.2	8.2	3.6	3.1
Tuscaloosa, AL	13.7	8.0	3.5	1.2
San Antonio, TX	2.9	1.2	0.3	0.6
Orlando, FL	5.3	1.9	0.4	0.2

Similar to previous works on severe weather climatology, it is also important to understand the temporal distributions of SCS climatology. Thus, cumulative frequencies of mean of PPH “slight” events were calculated for each city (Fig. 8a). Cumulative counts of PPH “slight” risk events reveal some known (e.g., Brooks et al. 2003) aspects about the timing of peak SCS frequency in the United States. For example, Bismarck experiences a focused threat for 5% PPH tornado events from \approx 1 June to 1 September, whereas the annual 5% PPH tornado counts in Tuscaloosa display a near-linear accumulation (Fig. 8b). Additional annual accumulation graphics are shown for 15% PPH hail and 15% PPH wind events (Figs. 8c,d, respectively).

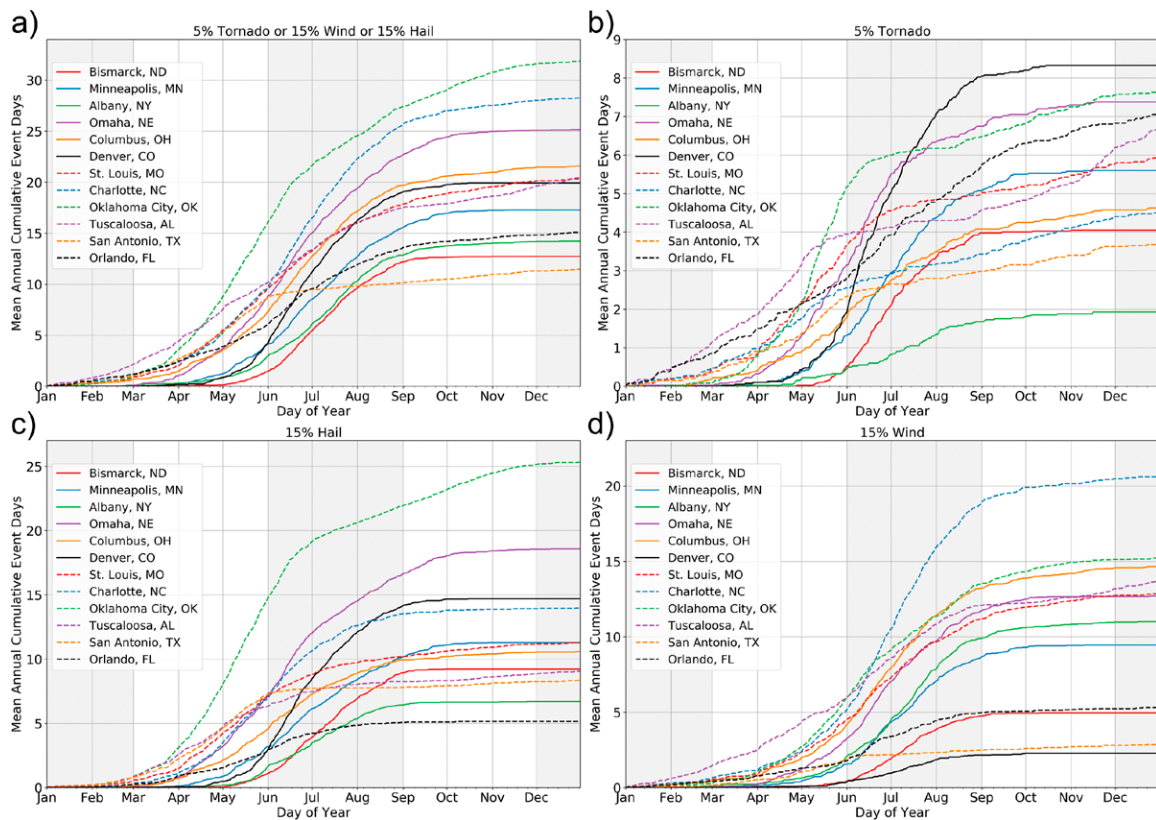


Fig. 8. Mean annual cumulative frequency of days (1200–1200 UTC) meeting or exceeding a practically perfect probability of (a) 5% for tornado, 15% for hail, or 15% for wind, (b) 5% for tornado, (c) 15% for hail, and (d) 15% for wind reports.

Top-10 coverage days. Areal coverage of PPH thresholds were used to rank the top-10 events for each SCS hazard during the period 1979–2018. For tornadoes, 1200 UTC 27–1200 UTC 28 April 2011 ranked as the top event (Table 4). Interestingly, the day before ranked as the second largest coverage event for both the 30% and 45% thresholds. Several other major historical tornado outbreaks were noted in the top-10 45% and 10% significant tornado PPH threshold coverages.

The same analysis was conducted for large hail (Table 5) and damaging convective wind gusts (Table 6). Remarkably, all top-10 events for each hail threshold have happened since 2002, and for 10% significant hail, all 10 have occurred since 2008. The top areal coverage day for 15%, 30%, and 60% PPH hail thresholds was 22 June 2008. On this day, 374 severe hail reports were recorded across the United States, with a majority (196) of reports occurring in North Carolina, Virginia, West Virginia, Ohio, and Indiana.

Top-10 spatial extents for 15%, 30%, and 60% PPH convective wind gust events have all occurred since 2004, again underscoring the recent increases in reporting (Table 6). In addition, eight out of the top-ten 10% PPH “hatching” events have occurred since 2011, with the

Table 4. The top 10 days (1200–1200 UTC) ranked by total area (10^6 km^2) meeting or exceeding selected practically perfect probability thresholds for tornadoes.

Rank	5% tornado	30% tornado	45% tornado	10% significant tornado
1	27 Apr 2011 (1.64)	27 Apr 2011 (0.8352)	27 Apr 2011 (0.6336)	27 Apr 2011 (0.672)
2	25 May 2011 (1.4528)	26 Apr 2011 (0.6224)	26 Apr 2011 (0.5024)	26 Apr 1991 (0.5504)
3	30 May 2004 (1.3088)	25 May 2011 (0.5744)	4 May 2003 (0.4384)	13 Mar 1990 (0.544)
4	26 Apr 1994 (1.3056)	30 May 2004 (0.568)	5 May 2007 (0.4192)	4 May 2003 (0.5024)
5	6 May 2003 (1.256)	4 May 2003 (0.5424)	30 May 2004 (0.3984)	7 Jun 1984 (0.488)
6	2 Apr 1982 (1.2512)	5 May 2007 (0.536)	25 May 2011 (0.3696)	2 Mar 2012 (0.4784)
7	26 Apr 2011 (1.2416)	5 Feb 2008 (0.4784)	5 Feb 2008 (0.3664)	22 Nov 1992 (0.4656)
8	8 Jun 1993 (1.208)	29 May 2004 (0.4752)	21 Jan 1999 (0.3616)	10 Nov 2002 (0.464)
9	10 Nov 2002 (1.2064)	10 Nov 2002 (0.4672)	23 Nov 2004 (0.3536)	2 Apr 1982 (0.4608)
10	21 Jun 1981 (1.168)	23 Nov 2004 (0.4656)	17 Jun 2010 (0.3488)	5 Feb 2008 (0.4352)

Table 5. As in Table 4, but for hail.

Rank	15% hail	30% hail	60% hail	10% significant hail
1	22 Jun 2008 (2.5888)	22 Jun 2008 (2.0048)	22 Jun 2008 (1.3232)	22 May 2011 (0.7824)
2	6 Jun 2005 (2.4752)	15 Jun 2009 (1.6816)	9 May 2003 (1.224)	27 May 2017 (0.6848)
3	22 Jul 2008 (2.352)	25 May 2008 (1.5888)	21 May 2004 (1.1872)	25 May 2011 (0.6272)
4	31 May 2008 (2.264)	6 Jun 2005 (1.5856)	15 Jun 2009 (1.1792)	25 May 2008 (0.5856)
5	19 Jun 2008 (2.224)	4 Jun 2002 (1.584)	2 Apr 2006 (1.1456)	2 Mar 2012 (0.5712)
6	20 Jun 2008 (2.2112)	24 May 2004 (1.5824)	7 Apr 2006 (1.1392)	17 Jun 2009 (0.5712)
7	17 Jun 2009 (2.192)	21 May 2004 (1.5808)	25 May 2008 (1.1376)	3 Jun 2014 (0.5696)
8	15 Jun 2009 (2.1904)	22 May 2011 (1.56)	22 May 2011 (1.0912)	2 Jun 2008 (0.5664)
9	4 Jun 2002 (2.1552)	9 May 2003 (1.5552)	8 May 2005 (1.0688)	10 May 2011 (0.5648)
10	10 Jun 2008 (2.1504)	17 Jun 2009 (1.5504)	3 Apr 2007 (1.0544)	9 Apr 2011 (0.5504)

Table 6. As in Table 4, but for wind.

Rank	15% wind	30% wind	60% wind	10% significant wind
1	6 Jul 2016 (2.6112)	4 Apr 2011 (2.0512)	4 Apr 2011 (1.744)	28 Jun 2018 (1.016)
2	22 Jul 2008 (2.56)	6 Jul 2016 (2.0176)	6 Jul 2016 (1.4592)	29 Jun 2012 (0.9696)
3	6 Jun 2005 (2.5568)	21 Jun 2011 (1.8144)	21 Jun 2011 (1.3504)	4 Apr 2011 (0.8768)
4	14 Jul 2016 (2.3504)	22 Jul 2008 (1.7632)	28 Jun 2018 (1.3248)	19 Apr 2011 (0.7712)
5	4 Apr 2011 (2.3344)	1 Jul 2012 (1.7616)	1 Jul 2012 (1.312)	30 May 1998 (0.7328)
6	1 Jul 2012 (2.2976)	28 Jun 2018 (1.7264)	30 May 2004 (1.2656)	30 Jun 2014 (0.7136)
7	28 Jul 2006 (2.2592)	22 Jun 2006 (1.712)	17 Jun 2016 (1.1936)	17 Jun 2016 (0.6768)
8	30 Jun 2015 (2.2336)	14 Jul 2016 (1.6432)	29 Jun 2012 (1.088)	6 Mar 2017 (0.6752)
9	4 Jul 2012 (2.2144)	17 Jun 2016 (1.6336)	22 Jun 2006 (1.0688)	10 Jul 2011 (0.6496)
10	9 Aug 2012 (2.1744)	28 Jul 2006 (1.6304)	24 Jun 2018 (1.0656)	18 Jun 1998 (0.6368)

other two events recorded during the notable derecho frequency period of May–June 1998 (Ashley et al. 2007). The largest area of 60% PPH wind probabilities was recorded on 4 April 2011, when over 1,000 damaging convective wind gusts were reported across the southeastern United States in association with a quasi-linear convective system.

Daily areal PPH coverage were also accumulated for each year (1979–2018) using the “slight” risk threshold (Fig. 9). For tornadoes, the maximum annual cumulative coverage meeting or exceeding a PPH value of 5% was in 2004 ($4.1 \times 10^7 \text{ km}^2$). The minimum value of $2 \times 10^7 \text{ km}^2$ was

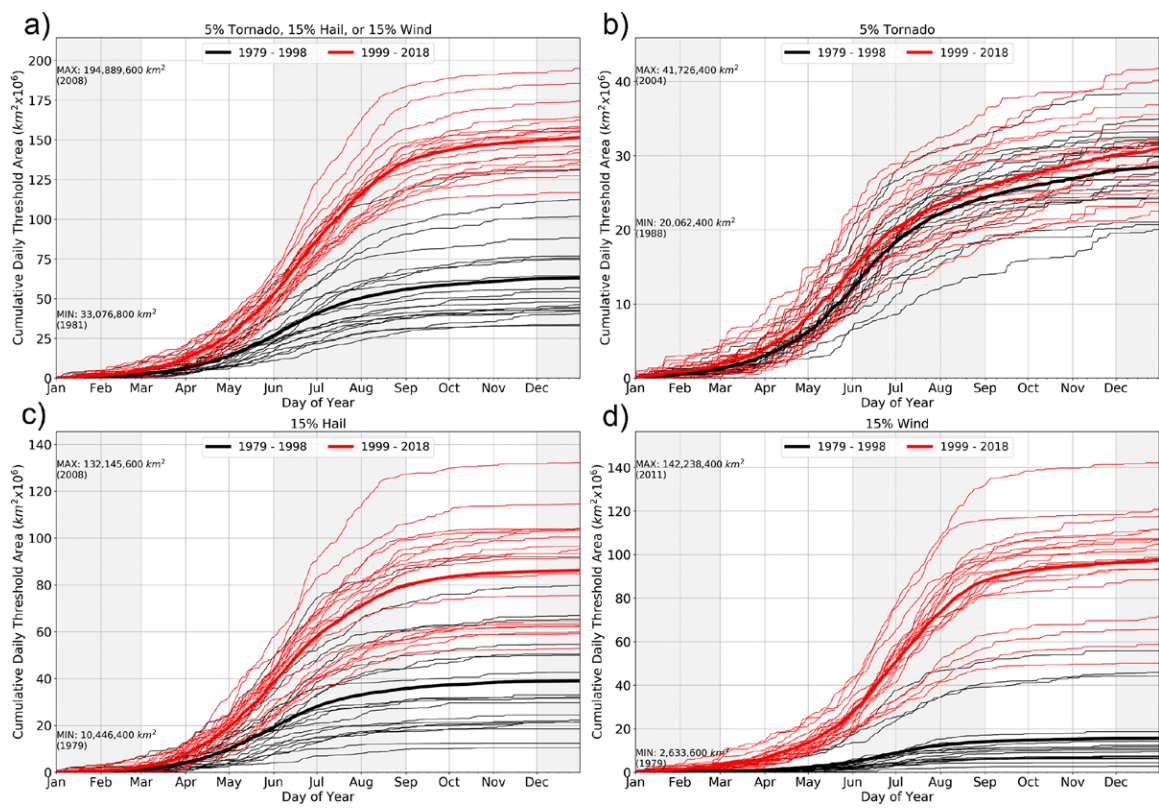


Fig. 9. Annual cumulative daily (1200–1200 UTC) area (10^6 km^2) exceeding a practically perfect probability of (a) 5% for tornado, 15% for hail, or 15% for wind, (b) 5% for tornado, (c) 15% for hail, and (d) 15% for wind. The thicker lines denote the mean for each of the epochs; namely, 1979–98 (black) and 1999–2018 (red).

recorded in 1988, which was likely due to the significant drought conditions present during late spring through summer 1988 across the central plains (Fig. 9b). On average, cumulative coverages for tornadoes slightly increased between the two epochs, but the increase was not statistically significant. For hail (Fig. 9c) and especially wind (Fig. 9d), dramatically large increases are found in the cumulative areal “slight” risk coverages between the two 20-yr epochs. Both hail and wind minimums were recorded in 1979, with maximums in 2008 and 2011, respectively. Cumulative daily coverage area by year (broken down for each epoch) is shown in Tables 7 and 8. This helps to summarize a doubling in hail report coverage and a quadrupling of wind report coverage over the course of the study period. Thus, we caution all readers to understand that the latest “modern” era in consistent reporting for all hazards began around the year 1996.

Summary and conclusions

A modern climatology of U.S. severe convective storm reports was presented and examined for the 40-yr period 1979–2018. Reports were examined daily and smoothed using a Gaussian kernel to calculate practically perfect hindcasts following an established forecast product definition from the NOAA/NWS’s Storm Prediction Center (SPC). Climatologies of these practically perfect hindcasts were analyzed at the “slight,” “moderate,” and “hatching” categorical thresholds used by the SPC that correspond to specific practically perfect hazard probability thresholds. Overall, spatial patterns of tornadoes, large hail, and damaging convective wind gust probabilities did not differ significantly from previous research examining aspects of severe weather climatology. Spatial changes in tornado probabilities were found between two 20-yr epochs, with increases found in the middle Mississippi Valley region and decreases in portions of the High Plains and southern Great Plains. Similar results were found in recent

Table 7. Yearly cumulative daily coverage area (10^6 km^2) from 1979 to 1998 for 5% tornado, 15% hail, 15% wind, and daily combined coverage of these thresholds ordered from highest to lowest annual combined area.

Year	5% tornado	15% hail	15% wind	5% tornado, 15% hail, or 15% wind
1998	38.4352	91.9120	55.7184	130.9632
1996	32.2864	79.6976	45.8320	112.3840
1997	31.4368	66.8592	44.1424	101.8272
1995	31.7168	65.1616	18.6336	88.2656
1994	29.9264	54.5568	15.9040	76.8368
1992	34.9104	50.5344	14.1344	75.7904
1993	33.2128	49.9024	15.6000	74.6832
1991	32.4896	42.5536	11.7408	64.5184
1990	31.6064	32.2016	10.8016	56.9552
1989	25.3424	32.9536	12.3312	54.3808
1986	24.4560	29.6688	7.1696	50.3360
1985	21.0608	31.5584	6.0800	47.9824
1982	29.8080	22.1968	6.5424	46.3888
1983	27.6736	21.3952	7.1504	44.6672
1984	26.8384	24.4464	6.6256	44.1072
1980	26.7344	18.5440	10.2160	42.6848
1987	20.6992	21.2512	9.4256	42.1872
1988	20.0624	21.4272	7.4272	40.5904
1979	25.9936	10.4464	2.6336	33.7504
1981	24.1760	12.3808	4.3104	33.0768
Mean	28.4433	38.9824	15.6210	63.1188

Table 8. As in Table 7, but for 1999–2018.

Year	5% tornado	15% hail	15% wind	5% tornado, 15% hail, or 15% wind
2008	40.1568	132.1456	120.8688	194.8896
2011	36.8208	93.2800	142.2384	185.5920
2006	27.7408	114.4592	106.9200	174.4608
2007	28.8736	103.9792	102.1984	164.3680
2005	30.9072	104.1904	93.5120	162.4592
2009	31.8208	103.7792	98.2160	158.2960
2004	41.7264	100.3904	88.3936	157.4720
2010	32.4880	64.7952	118.0224	156.4432
2003	32.1968	103.2640	93.2272	155.3584
2012	22.5200	75.4464	111.5440	154.7792
2016	26.5152	62.4048	111.4768	150.7936
2017	35.5520	63.2384	107.4768	146.0928
2015	30.4784	59.8416	104.8240	143.8784
2018	29.2432	52.8064	106.8944	142.2144
2001	31.9392	96.3760	65.4800	137.5232
2002	25.2352	95.3888	71.7984	136.3872
2013	23.7024	62.1488	98.7312	134.4304
2014	25.3520	59.1232	97.4480	131.5296
2000	31.3200	91.4048	58.6624	127.4352
1999	33.9856	84.8336	50.0896	116.8880
Mean	30.9287	86.1648	97.4011	151.5646

research by Gensini and Brooks (2018). Hail reports were found to increase over a majority of the CONUS (especially in portions of Kansas, Nebraska, and South Dakota), while damaging convective wind gusts saw the greatest increases between the two epochs, especially across the eastern third of the CONUS. Of the three natural hazards, tornadoes exhibited the least amount of change through the study period. Hail increased through the analysis years by a factor of 2, while wind increased by a factor of 4 using both counts and coverage metrics. Significant severe weather was less impacted by such trends. The authors recommend that interested users of the severe weather database understand that the latest “modern” era in consistent reporting for all hazards began in 1996.

Finally, data examined herein are available to interested readers in an effort to create an open-source repository for SCS climatological studies wishing to use the practically perfect hindcasts. netCDF files used for this study are available for download at <http://atlas.niu.edu/pperfect/BAMS> or by contacting the corresponding author. In addition, sample Python code notebooks for plotting and analysis of the files are available via the open source GitHub repository (https://github.com/ahaberlie/PPer_Climo).

Acknowledgments. The authors wish to thank Drs. Nathan Hitchens, Kimberly Hoogewind, and Harold Brooks for their comments on an initial draft of this manuscript.

References

- Allen, J. T., and M. K. Tippett, 2015: The characteristics of United States hail reports: 1955–2014. *Electron. J. Severe Storms Meteor.*, **10** (3), www.ejssm.org/ojs/index.php/ejssm/article/viewArticle/149.
- , —, and A. H. Sobel, 2015: An empirical model relating US monthly hail occurrence to large-scale meteorological environment. *J. Adv. Model. Earth Syst.*, **7**, 226–243, https://doi.org/10.1002/2014MS000397.
- Ashley, W. S., and T. L. Mote, 2005: Derecho hazards in the United States. *Bull. Amer. Meteor. Soc.*, **86**, 1577–1592, https://doi.org/10.1175/BAMS-86-11-1577.
- , —, and S. M. Strader, 2016: Recipe for disaster: How the dynamic ingredients of risk and exposure are changing the tornado disaster landscape. *Bull. Amer. Meteor. Soc.*, **97**, 767–786, https://doi.org/10.1175/BAMS-D-15-00150.1.
- , T. L. Mote, and M. L. Bentley, 2007: The extensive episode of derecho-producing convective systems in the United States during May and June 1998: A multi-scale analysis and review. *Meteor. Appl.*, **14**, 227–244, https://doi.org/10.1002/met.23.
- , S. Strader, T. Rosencrants, and A. J. Krmenec, 2014: Spatiotemporal changes in tornado hazard exposure: The case of the expanding bull's-eye effect in Chicago, Illinois. *Wea. Climate Soc.*, **6**, 175–193, https://doi.org/10.1175/WCAS-D-13-00047.1.
- Banacos, P. C., and M. L. Ekster, 2010: The association of the elevated mixed layer with significant severe weather events in the northeastern United States. *Wea. Forecasting*, **25**, 1082–1102, https://doi.org/10.1175/2010WAF222363.1.
- Bentley, M. L., and T. L. Mote, 1998: A climatology of derecho-producing mesoscale convective systems in the central and eastern United States, 1986–95. Part I: Temporal and spatial distribution. *Bull. Amer. Meteor. Soc.*, **79**, 2527–2540, https://doi.org/10.1175/1520-0477(1998)079<2527:ACODPM>2.0.CO;2.
- , —, 2000: A synoptic climatology of cool-season derecho events. *Phys. Geogr.*, **21**, 21–37, https://doi.org/10.1080/02723646.2000.10642696.
- Brimelow, J. C., W. R. Burrows, and J. M. Hanesiak, 2017: The changing hail threat over North America in response to anthropogenic climate change. *Nat. Climate Change*, **7**, 516–522, https://doi.org/10.1038/nclimate3321.
- Brooks, H. E., 2013: Severe thunderstorms and climate change. *Atmos. Res.*, **123**, 129–138, https://doi.org/10.1016/j.atmosres.2012.04.002.
- , —, and N. Dotzek, 2008: The spatial distribution of severe convective storms and an analysis of their secular changes. *Climate Extremes and Society*, H. F. Diaz and R. J. Murnane, Eds., Cambridge University Press, 35–53.
- , C. A. Doswell III, and J. Cooper, 1994: On the environments of tornadic and nontornadic mesocyclones. *Wea. Forecasting*, **9**, 606–618, https://doi.org/10.1175/1520-0434(1994)009<0606:OTEOTA>2.0.CO;2.
- , —, and M. P. Kay, 2003: Climatological estimates of local daily tornado probability for the United States. *Wea. Forecasting*, **18**, 626–640, https://doi.org/10.1175/1520-0434(2003)018<0626:CEOLDT>2.0.CO;2.
- , G. W. Carbin, and P. T. Marsh, 2014: Increased variability of tornado occurrence in the United States. *Science*, **346**, 349–352, https://doi.org/10.1126/science.1257460.
- Carlson, T., S. Benjamin, G. Forbes, and Y. Li, 1983: Elevated mixed layers in the regional severe storm environment: Conceptual model and case studies. *Mon. Wea. Rev.*, **111**, 1453–1474, https://doi.org/10.1175/1520-0493(1983)111<1453:EMLTR>2.0.CO;2.
- Cecil, D. J., and C. B. Blankenship, 2012: Toward a global climatology of severe hailstorms as estimated by satellite passive microwave imagers. *J. Climate*, **25**, 687–703, https://doi.org/10.1175/JCLI-D-11-00130.1.
- Changnon, S. A., 1977: The scales of hail. *J. Appl. Meteor.*, **16**, 626–648, https://doi.org/10.1175/1520-0450(1977)016<0626:TSOH>2.0.CO;2.
- , 1999: Data and approaches for determining hail risk in the contiguous United States. *J. Appl. Meteor.*, **38**, 1730–1739, https://doi.org/10.1175/1520-0450(1999)038<1730:DAAFDH>2.0.CO;2.
- , 2001: Damaging thunderstorm activity in the United States. *Bull. Amer. Meteor. Soc.*, **82**, 597–608, https://doi.org/10.1175/1520-0477(2001)082<0597:DTAITU>2.3.CO;2.
- , 2008: Temporal and spatial distributions of damaging hail in the continental United States. *Phys. Geogr.*, **29**, 341–350, https://doi.org/10.2747/0272-3646.29.4.341.
- , —, and D. Changnon, 2000: Long-term fluctuations in hail incidences in the United States. *J. Climate*, **13**, 658–664, https://doi.org/10.1175/1520-0442(2000)013<0658:LTFIHI>2.0.CO;2.
- Cheng, V. Y., G. B. Arhonditsis, D. M. Sills, W. A. Gough, and H. Auld, 2016: Predicting the climatology of tornado occurrences in North America with a Bayesian hierarchical modeling framework. *J. Climate*, **29**, 1899–1917, https://doi.org/10.1175/JCLI-D-15-0404.1.
- Cintineo, J. L., T. M. Smith, V. Lakshmanan, H. E. Brooks, and K. L. Ortega, 2012: An objective high-resolution hail climatology of the contiguous United States. *Wea. Forecasting*, **27**, 1235–1248, https://doi.org/10.1175/WAF-D-11-00151.1.
- Coniglio, M. C., and D. J. Stensrud, 2004: Interpreting the climatology of derechos. *Wea. Forecasting*, **19**, 595–605, https://doi.org/10.1175/1520-0434(2004)019<0595:ITCOD>2.0.CO;2.
- Del Genio, A. D., M.-S. Yao, and J. Jonas, 2007: Will moist convection be stronger in a warmer climate? *Geophys. Res. Lett.*, **34**, L16703, https://doi.org/10.1029/2007GL030525.
- Diffenbaugh, N. S., M. Scherer, and R. J. Trapp, 2013: Robust increases in severe thunderstorm environments in response to greenhouse forcing. *Proc. Natl. Acad. Sci. USA*, **110**, 16 361–16 366, https://doi.org/10.1073/pnas.1307758110.
- Doswell, C. A., H. E. Brooks, and N. Dotzek, 2009: On the implementation of the enhanced Fujita scale in the USA. *Atmos. Res.*, **93**, 554–563, https://doi.org/10.1016/j.atmosres.2008.11.003.
- Edwards, R., J. T. Allen, and G. W. Carbin, 2018: Reliability and climatological impacts of convective wind estimations. *J. Appl. Meteor. Climatol.*, **57**, 1825–1845, https://doi.org/10.1175/JAMC-D-17-0306.1.
- Farney, T. J., and P. G. Dixon, 2015: Variability of tornado climatology across the continental United States. *Int. J. Climatol.*, **35**, 2993–3006, https://doi.org/10.1002/joc.4188.
- Ferguson, A. P., and W. S. Ashley, 2017: Spatiotemporal analysis of residential flood exposure in the Atlanta, Georgia metropolitan area. *Nat. Hazards*, **87**, 989–1016, https://doi.org/10.1007/s11069-017-2806-6.
- Freeman, A. C., and W. S. Ashley, 2017: Changes in the US hurricane disaster landscape: The relationship between risk and exposure. *Nat. Hazards*, **88**, 659–682, https://doi.org/10.1007/s11069-017-2885-4.
- Gensini, V. A., and W. L. Ashley, 2011: Climatology of potentially severe convective environments from the North American regional reanalysis. *Electron. J. Severe Storms Meteor.*, **6** (8), www.ejssm.org/ojs/index.php/ejssm/article/viewArticle/85.
- , and T. L. Mote, 2015: Downscaled estimates of late 21st century severe weather from CCSM3. *Climatic Change*, **129**, 307–321, https://doi.org/10.1007/s10584-014-1320-z.
- , and H. E. Brooks, 2018: Spatial trends in United States tornado frequency. *npg Climate Atmos. Sci.*, **1**, 38, https://doi.org/10.1038/S41612-018-0048-2.
- , and L. Bravo de Guenni, 2019: Environmental covariate representation of seasonal US tornado frequency. *J. Appl. Meteor. Climatol.*, **58**, 1353–1367, https://doi.org/10.1175/JAMC-D-18-0305.1.
- , and M. K. Tippett, 2019: Global Ensemble Forecast System (GEFS) predictions of days 1–15 US tornado and hail frequencies. *Geophys. Res. Lett.*, **46**, 2922–2930, https://doi.org/10.1029/2018GL081724.
- , C. Ramseyer, and T. L. Mote, 2014: Future convective environments using NARCCAP. *Int. J. Climatol.*, **34**, 1699–1705, https://doi.org/10.1002/joc.3769.
- Guo, L., K. Wang, and H. B. Bluestein, 2016: Variability of tornado occurrence over the continental United States since 1950. *J. Geophys. Res. Atmos.*, **121**, 6943–6953, https://doi.org/10.1002/2015JD024465.
- Hitchens, N. M., and H. E. Brooks, 2012: Evaluation of the Storm Prediction Center's day 1 convective outlooks. *Wea. Forecasting*, **27**, 1580–1585, https://doi.org/10.1175/WAF-D-12-00061.1.

- , and —, 2014: Evaluation of the Storm Prediction Center's convective outlooks from day 3 through day 1. *Wea. Forecasting*, **29**, 1134–1142, <https://doi.org/10.1175/WAF-D-13-00132.1>.
- , —, and M. P. Kay, 2013: Objective limits on forecasting skill of rare events. *Wea. Forecasting*, **28**, 525–534, <https://doi.org/10.1175/WAF-D-12-00113.1>.
- Hoogewind, K. A., M. E. Baldwin, and R. J. Trapp, 2017: The impact of climate change on hazardous convective weather in the United States: Insight from high-resolution dynamical downscaling. *J. Climate*, **30**, 10081–10100, <https://doi.org/10.1175/JCLI-D-16-0885.1>.
- Idso, S., R. Ingram, and J. Pritchard, 1972: An American haboob. *Bull. Amer. Meteor. Soc.*, **53**, 930–935, [https://doi.org/10.1175/1520-0477\(1972\)053<0930:AAH>2.0.CO;2](https://doi.org/10.1175/1520-0477(1972)053<0930:AAH>2.0.CO;2).
- Jewell, R., and J. Brimelow, 2009: Evaluation of Alberta hail growth model using severe hail proximity soundings from the United States. *Wea. Forecasting*, **24**, 1592–1609, <https://doi.org/10.1175/2009WAF2222230.1>.
- Kelly, D., J. Schaefer, R. McNulty, C. Doswell III, and R. Abbey Jr., 1978: An augmented tornado climatology. *Mon. Wea. Rev.*, **106**, 1172–1183, [https://doi.org/10.1175/1520-0493\(1978\)106<1172:AATC>2.0.CO;2](https://doi.org/10.1175/1520-0493(1978)106<1172:AATC>2.0.CO;2).
- Krocak, M. J., and H. E. Brooks, 2018: Climatological estimates of hourly tornado probability for the United States. *Wea. Forecasting*, **33**, 59–69, <https://doi.org/10.1175/WAF-D-17-0123.1>.
- Kunkel, K. E., and Coauthors, 2013: Monitoring and understanding trends in extreme storms: State of knowledge. *Bull. Amer. Meteor. Soc.*, **94**, 499–514, <https://doi.org/10.1175/BAMS-D-11-00262.1>.
- Lanicci, J. M., and T. T. Warner, 1991: A synoptic climatology of the elevated mixed-layer inversion over the southern Great Plains in spring. Part II: The life cycle of the lid. *Wea. Forecasting*, **6**, 198–213, [https://doi.org/10.1175/1520-0434\(1991\)006<0198:ASCOTE>2.0.CO;2](https://doi.org/10.1175/1520-0434(1991)006<0198:ASCOTE>2.0.CO;2).
- , and —, 1997: A case study of lid evolution using analyses of observational data and a numerical model simulation. *Wea. Forecasting*, **12**, 228–252, [https://doi.org/10.1175/1520-0434\(1997\)012<0228:ACSOLE>2.0.CO;2](https://doi.org/10.1175/1520-0434(1997)012<0228:ACSOLE>2.0.CO;2).
- Long, J. A., P. C. Stoy, and T. Gerken, 2018: Tornado seasonality in the southeastern United States. *Wea. Climate Extremes*, **20**, 81–91, <https://doi.org/10.1016/j.wace.2018.03.002>.
- Marsh, P. T., H. E. Brooks, and D. J. Karoly, 2007: Assessment of the severe weather environment in North America simulated by a global climate model. *Atmos. Sci. Lett.*, **8**, 100–106, <https://doi.org/10.1002/asl.159>.
- Moore, T. W., and T. A. DeBoer, 2019: A review and analysis of possible changes to the climatology of tornadoes in the United States. *Prog. Phys. Geogr. Earth Environ.*, **43**, 365–390, <https://doi.org/10.1177/0309133319829398>.
- , and M. P. McGuire, 2019: Using the standard deviational ellipse to document changes to the spatial dispersion of seasonal tornado activity in the United States. *npj Climate Atmos. Sci.*, **2**, 21, <https://doi.org/10.1038/S41612-019-0078-4>.
- NCEI, 2020: U.S. billion-dollar weather and climate disasters. NOAA, accessed January 2019, www.ncdc.noaa.gov/billions/.
- Potvin, C. K., C. Broyles, P. S. Skinner, H. E. Brooks, and E. Rasmussen, 2019: A Bayesian hierarchical modeling framework for correcting reporting bias in the U.S. tornado database. *Wea. Forecasting*, **34**, 15–30, <https://doi.org/10.1175/WAF-D-18-0137.1>.
- Rosencrants, T. D., and W. S. Ashley, 2015: Spatiotemporal analysis of tornado exposure in five US metropolitan areas. *Nat. Hazards*, **78**, 121–140, <https://doi.org/10.1007/s11069-015-1704-z>.
- Schaefer, J. T., and R. Edwards, 1999: The SPC tornado/severe thunderstorm database. Preprints, *11th Conf. Applied Climatology*, Dallas, TX, Amer. Meteor. Soc., 215–220.
- Simmons, K., and D. Sutter, 2013: *Economic and Societal Impacts of Tornadoes*. Springer Science and Business, 296 pp.
- Smith, A. B., and J. L. Matthews, 2015: Quantifying uncertainty and variable sensitivity within the US billion-dollar weather and climate disaster cost estimates. *Nat. Hazards*, **77**, 1829–1851, <https://doi.org/10.1007/s11069-015-1678-x>.
- Smith, B. T., T. E. Castellanos, A. C. Winters, C. M. Mead, A. R. Dean, and R. L. Thompson, 2013: Measured severe convective wind climatology and associated convective modes of thunderstorms in the contiguous United States, 2003–09. *Wea. Forecasting*, **28**, 229–236, <https://doi.org/10.1175/WAF-D-12-00096.1>.
- Strader, S. M., 2018: Spatiotemporal changes in conterminous US wildfire exposure from 1940 to 2010. *Nat. Hazards*, **92**, 543–565, <https://doi.org/10.1007/s11069-018-3217-z>.
- , and W. S. Ashley, 2015: The expanding bull's-eye effect. *Weatherwise*, **68**, 23–29, <https://doi.org/10.1080/00431672.2015.1067108>.
- , —, T. J. Pingel, and A. J. Krmenec, 2017a: Observed and projected changes in United States tornado exposure. *Wea. Climate Soc.*, **9**, 109–123, <https://doi.org/10.1175/WCAS-D-16-0041.1>.
- , —, —, and —, 2017b: Projected 21st century changes in tornado exposure, risk, and disaster potential. *Climatic Change*, **141**, 301–313, <https://doi.org/10.1007/s10584-017-1905-4>.
- Tang, B. H., V. A. Gensini, and C. R. Homeyer, 2019: Trends in United States large hail environments and observations. *npj Climate Atmos. Sci.*, **2**, 45, <https://doi.org/10.1038/S41612-019-0103-7>.
- Thom, H., 1963: Tornado probabilities. *Mon. Wea. Rev.*, **91**, 730–736, [https://doi.org/10.1175/1520-0493\(1963\)091<0730:TP>2.3.CO;2](https://doi.org/10.1175/1520-0493(1963)091<0730:TP>2.3.CO;2).
- Tippett, M. K., 2014: Changing volatility of US annual tornado reports. *Geophys. Res. Lett.*, **41**, 6956–6961, <https://doi.org/10.1002/2014GL061347>.
- , A. H. Sobel, and S. J. Camargo, 2012: Association of U.S. tornado occurrence with monthly environmental parameters. *Geophys. Res. Lett.*, **39**, L02801, <https://doi.org/10.1029/2011GL050368>.
- , —, —, and J. T. Allen, 2014: An empirical relation between us tornado activity and monthly environmental parameters. *J. Climate*, **27**, 2983–2999, <https://doi.org/10.1175/JCLI-D-13-00345.1>.
- , J. T. Allen, V. A. Gensini, and H. E. Brooks, 2015: Climate and hazardous convective weather. *Curr. Climate Change Rep.*, **1**, 60–73, <https://doi.org/10.1007/s40641-015-0006-6>.
- Trapp, R. J., and K. A. Hoogewind, 2016: The realization of extreme tornadic storm events under future anthropogenic climate change. *J. Climate*, **29**, 5251–5265, <https://doi.org/10.1175/JCLI-D-15-0623.1>.
- , D. M. Wheatley, N. T. Atkins, R. W. Przybylinski, and R. Wolf, 2006: Buyer beware: Some words of caution on the use of severe wind reports in postevent assessment and research. *Wea. Forecasting*, **21**, 408–415, <https://doi.org/10.1175/WAF925.1>.
- , N. S. Diffenbaugh, H. E. Brooks, M. E. Baldwin, E. D. Robinson, and J. S. Pal, 2007: Changes in severe thunderstorm environment frequency during the 21st century caused by anthropogenically enhanced global radiative forcing. *Proc. Natl. Acad. Sci. USA*, **104**, 19719–19723, <https://doi.org/10.1073/pnas.0705494104>.
- , K. A. Hoogewind, and S. Lasher-Trapp, 2019: Future changes in hail occurrence in the United States determined through convection-permitting dynamical downscaling. *J. Climate*, **32**, 5493–5509, <https://doi.org/10.1175/JCLI-D-18-0740.1>.
- Verbout, S. M., H. E. Brooks, L. M. Leslie, and D. M. Schultz, 2006: Evolution of the U.S. tornado database: 1954–2003. *Wea. Forecasting*, **21**, 86–93, <https://doi.org/10.1175/WAF910.1>.